ACI STRUCTURAL JOURNAL TECHNICAL PAPER

Title no. 97-S62

Behavior of High-Strength Concrete Columns under Cyclic Flexure and Constant Axial Load

by Frédéric Légeron and Patrick Paultre

This paper presents the results of a study conducted on six large-scale columns made of high-strength concrete (HSC). The columns were subjected to constant axial loads corresponding to target values of 15, 25, and 40% of the column axial-load capacity and a cyclic horizontal load-inducing reversed bending moment. It is shown that tie spacing, and therefore tie volumetric ratio and axial-load level have significant effects on the flexural behavior of HSC columns. The need to include the axial-load level in code requirements for confinement reinforcement is pointed out.

Keywords: confined concrete; ductility; high-strength concrete; strength; tied column.

INTRODUCTION

High-strength concrete (HSC) is now readily available for various practical applications such as bridges, offshore platforms, and buildings, as a result of ongoing progress in concrete technology. HSC offers many advantages, including excellent mechanical performance and durability, that could result in initial and long-term cost reduction. HSC, however, is more brittle than conventional normal strength concrete (NSC). Current confinement requirements,[1] which were originally derived from experimental results on NSC, are not suited for HSC columns.[2-4]

Nonetheless, it has been shown that HSC columns can behave in a ductile manner under certain conditions.[2-5] Hence, ACI-ASCE Committee 441[6] pointed out that columns subjected to axial loads less than 20% of column axial-load capacity exhibited a good level of ductility when confined according to current ACI confinement requirements. The scientific community has not yet reached a consensus on required confinement reinforcement for ductile HSC columns. This can be explained by the limited number of tests on columns under cyclic flexure and significant axial compression, specifically with axial-load in the range of 20 to 40% of column axial-load capacity.[6] It has also been shown that the confinement mechanism was not described properly by existing models.[7] Therefore, in seismically active regions, structural engineers tend to avoid using HSC.

A comprehensive research program has been underway for the past decade to rationally model the confinement mechanism.[8,9] This research program includes extensive testing on large-scale columns,[8,9] as well as analytical studies. In the first part of this work, HSC columns were tested under concentric compression.[7] A confinement model, based on equilibrium and strain compatibility, has been developed and calibrated with available data.[8,9] To complement this work, tests on HSC columns subjected to combined constant axial-load and reversed cyclic flexure were performed. Four parameters are currently under study: 1) the level of axial compression; 2) the volumetric ratio of confinement steel; 3) the concrete strength; and 4) the yield strength of the confinement steel. This paper discusses the effects of the first two variables on the seismic behavior of HSC columns.

RESEARCH SIGNIFICANCE

This paper provides new test data pertaining to the seismic behavior of HSC columns. Six large-scale specimens were subjected to combined constant axial-load and reversed cyclic flexure. The target concrete strength was 100 MPa. The influence of two parameters are investigated: 1) the axial-load level; and 2) the volumetric ratio of confinement steel. The test data and recent results from HSC column tests obtained by other researchers are used to evaluate different equations that have been proposed for determination of confinement reinforcement for HSC columns located in seismic zones.

EXPERIMENTAL PROGRAM

Test specimens

The specimens tested in this research program consisted of full-size 305 x 305 x 2150 mm columns built monolithically to a massive I-shaped stub, and cast vertically. The stub represents a rigid member such as a beam-column joint or a slab foundation (Fig. 1 and 2). The transverse load is applied at the tip of the specimen, 2 m from the base of the column. The specimens represent a 4.0 m high column in a typical building, assuming that the point of contraflexure is located at midcolumn height. This corresponds to a height-width ratio of approximately 13, which was chosen to avoid shear-critical columns as this research program concentrates on flexural behavior. Figure 3 shows the specimen reinforcement detail and the tie configuration.

Test variables

The columns were designed to investigate the effects of two main parameters on their behavior: 1) the level of axial load; and 2) the volumetric ratio of confinement steel. The level of axial load is defined as the ratio of the applied constant axial compression P and the column concrete axial-load capacity $A_g f_c'$. The compressive force was applied at the tip of the column and kept constant at 1200, 2400, or 3600 kN. These loads correspond to a target axial-load level of 15, 25, or 40% of $A_g f_c'$, respectively. These values were selected to complete the available data on HSC columns. In addition, the three levels of axial load were intended to reflect the range of failure type: ductile, balanced, and fragile failure. A 15% axial-load level corresponds to a low level in which failure is reached by tensile

ACI Structural Journal, V. 97, No. 4, July-August 2000.
MS No. 99-127 received July 13, 1999, and reviewed under Institute publication policies. Pertinent discussion will be published in the May-June 2001 *ACI Structural Journal* if received by January 1, 2001.

ACI member **Frédéric Légeron** *is a bridge engineer in the large bridge division of SETRA, the technical center of the French Ministry of Transportation. He received his PhD from the University of Sherbrooke, Sherbrooke, Canada, and Ecole Nationale des Ponts et Chaussées in Paris. He is treasurer of the Paris ACI Chapter. His research interests include the seismic design of bridges, and the behavior, design, and nonlinear analysis of reinforced and prestressed concrete structures.*

ACI member **Patrick Paultre** *is a professor of structural engineering at the University of Sherbrooke. He is a member of Joint ACI-ASCE Committees 352, Joints and Connections in Monolithic Concrete Structures; and 441, Reinforced Concrete Columns.*

reinforcement yielding. A 40% axial-load level, generally considered as a high level, leads to crushing failure of the concrete. The 25% intermediate value corresponds to a balanced failure characterized by the simultaneous crushing of the concrete and the beginning of tensile reinforcement yielding.

Tie spacing and volumetric ratio are both important and interrelated parameters that control the ductility of tied-columns. Strictly, to investigate the influence of volumetric ratio of transverse reinforcement, tie spacing should instead be kept constant by varying tie diameter. Design codes usually refer to the ratio of tie cross section in a certain direction to tie spacing A_{sh}/s, with limits set on spacings. In this research program, both tie spacing and tie volumetric ratio are varied simultaneously as the specific influence of each parameter is not investigated, but the influence of volumetric ratio, accounted for by the total tie cross section in a certain direction A_{sh}, and the tie spacing s, are investigated. Hence, to investigate the influence of the volumetric ratio of confinement steel, the tie configuration was kept constant and the spacing of ties varied from 60 to 130 mm. A 130 mm tie spacing corresponds to a normal shear design controlled by the $d/2$ requirement in the ACI Code.[1] The 60 mm tie spacing was selected to obtain ductile behavior, even at high axial-load levels. It represents approximately 95% of the confinement steel required by the ACI Code.[1]

Test specimens are identified by concrete strength (C100), tie configuration (B) as used in Cusson and Paultre[7] for a square peripheral tie and an internal lozenge, tie spacing (60 or 130 mm), and the axial-load level (N15). Hence, C100B60N15 represents a column made of 100 MPa concrete with tie Configuration B, spaced at 60 mm, and subjected to a targeted axial-load level of 15% of $A_g f_c'$.

Material properties

Concrete—The specified 100 MPa concrete was mixed in the concrete laboratory. The concrete formulation was based

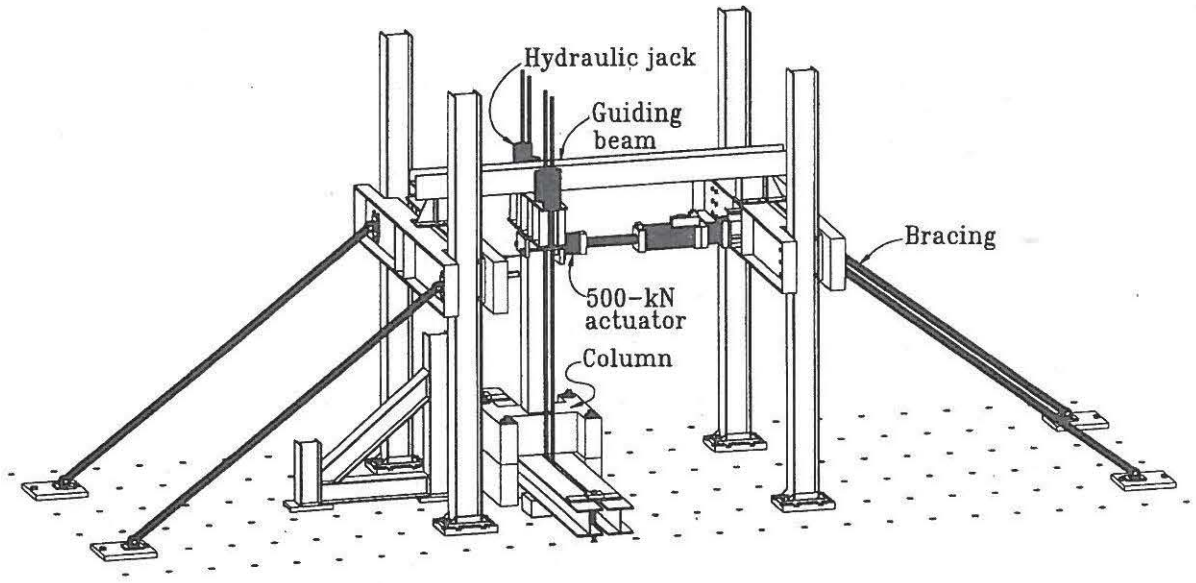

Fig. 1—Experimental setup.

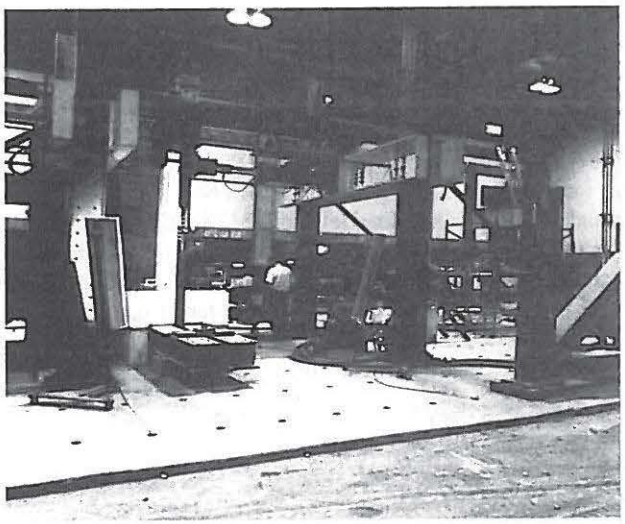

Fig. 2—Photograph of experimental setup and testing frame.

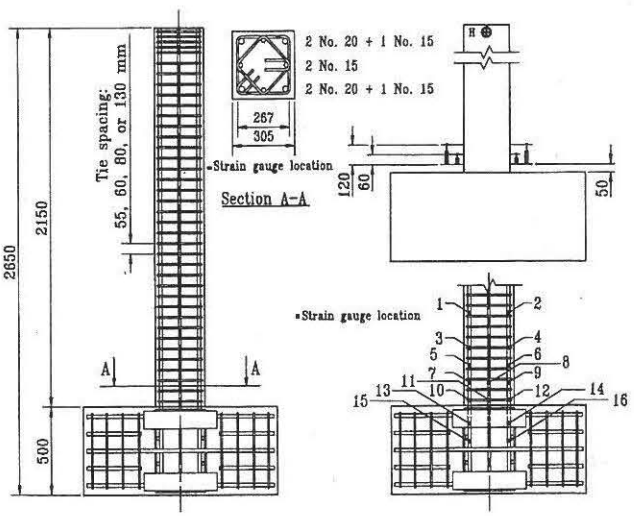

Fig. 3—Reinforcing cage and instrumentation details.

on a water-cement ratio (w/c) of 0.25. About 75% of the base stub was cast with one 1000 kg batch. A second batch of 1000 kg was used to complete the base stub and cast the column and the control specimens (cylinders and prisms). A retarding admixture was added to prevent the concrete from setting before the second batch was cast. The specimens were taken off the formwork the day after casting, covered with wet burlap, and wrapped in polythene sheets. The columns and stub faces were frequently watered to obtain good moist curing. Water demand was considerable, especially during the first week of curing. All the control cylinders and prisms were cured under the same conditions as the column specimens to estimate the column concrete material characteristics as accurately as possible.

Table 1 summarizes the measured material properties. The concrete compressive strength f_c' was determined from standard compressive tests on at least three 150 x 300 mm cylinders. Complete stress-strain curves were obtained from at least three 100 x 200 mm cylinders tested at a very slow rate in a very stiff rock testing machine. The postpeak strain at 50% of maximum stress ε_{c50u} was evaluated from the complete stress-strain curves obtained on 100 x 200 mm cylinders.

The average compressive strength ranged from 92.4 to 104.3 MPa. The secant modulus of elasticity E_c ranged from 34,300 to 41,000 MPa. The cracking strength of the concrete f_r, estimated from modulus of rupture tests on at least three 100 x 100 x 400 mm prisms for each specimen, ranged from 7.0 to 9.3 MPa.

Reinforcement—Three different types of metric reinforcing bars were used to construct the specimens: 10M (diameter d_b = 11.3 mm, cross-sectional area A_s = 100 mm^2), 15M (d_b = 16 mm, A_s = 200 mm^2), and 20M (d_b = 19.5 mm, A_s = 300 mm^2). Complete stress-strain curves were obtained from plain bar tests on each of the two batches of steel used. The averages of at least two steel coupons for each batch of steel are shown in Table 2, where f_y is the yield strength, ε_{sh} is the strain at the commencement of strain hardening, and ε_{su} is the ultimate strain corresponding to the ultimate stress f_{su}. All steels exhibited a well-defined yield plateau from the beginning of yielding to the commencement of strain hardening.

Reinforcing cages

Details of reinforcing cages are shown in Fig. 3. The longitudinal reinforcement for each specimen consisted of four No. 15M and four No. 20M Grade 400 deformed bars, providing a 2.15% longitudinal steel ratio (Fig. 3). No. 10M Grade 400 deformed bars were used as lateral reinforcement. To prevent crushing of the concrete, extra ties were placed at the top of the column where the axial load was applied. Elsewhere, ties were equally spaced. All ties were anchored with 135 degree bends extending 110 mm into the core, which exceeds the minimal length of six-bar diameters required by the ACI Code. No anchorage failure was observed during the test. The stub was designed to prevent excessive cracking and provide proper anchorage for the column's longitudinal bars.

Table 1—Concrete characteristics

Specimen	f_c', MPa	ε_c'	E_c, MPa	ε_{c50u}	f_r, MPa
C100B60N15	92.4	0.00290	41,000	—	7.80
C100B60N25	93.3	0.00331	36,400	0.00425	7.78
C100B60N40	98.2	0.00333	35,600	0.00433	8.33
C100B130N15	94.8	0.00290	41,000	—	7.80
C100B130N25	97.7	0.00352	34,300	0.00452	8.54
C100B130N40	104.3	0.00329	37,600	0.00410	9.04

Instrumentation and testing procedures

Sixteen electrical strain gages were placed in the specimens on the longitudinal bars above and in the stub (Fig. 3). Four sets of ties just above the stub were instrumented with 16 electrical strain gages. Curvatures were calculated from the strain gage measurements for the first two specimens tested (C100B60N15 and C100B130N15). As this type of measurement was not reliable during the full range of the test, curvatures were also calculated from the readings of two sets of four linear variable displacement transducers (LVDTs) for the other four specimens. The LVDTs were supported by steel rods passing through the core and extending from one side of the column to the other. These bars were attached to the longitudinal bars before concreting. Four LVDTs with a range of 5 mm were used to measure average concrete strain over a gage length of 60 mm. The other four LVDTs had a range of 25 mm, were placed over the four previous LVDTs, and were used to measure average concrete strain over a longer gage length of 120 mm (Fig. 3).

The column specimens were tested in a frame that was specifically designed for this research (Fig. 1). The axial compression in the column was applied through four high-strength, 36 mm diameter bars tensioned by two 1000 kN and two 1500 kN hydraulic jacks. Each bar was instrumented with strain gages to accurately determine the applied axial load. The horizontal load was applied by a 500 kN actuator, with displacement and force control capabilities, sup-

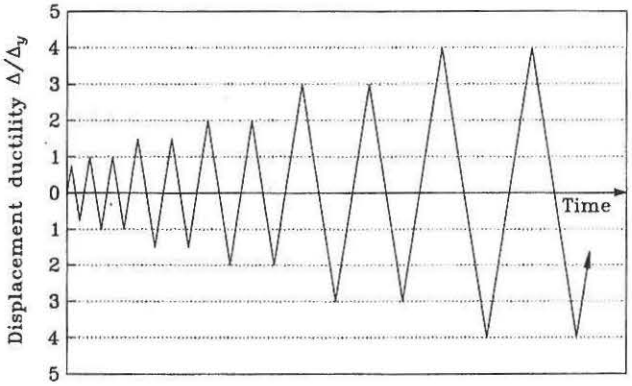

Fig. 4—Loading history.

Table 2—Steel characteristics

	No. 10				No. 15				No. 20			
Specimen	f_y, MPa	ε_{sh}	ε_{su}	f_{su}, MPa	f_y, MPa	ε_{sh}	ε_{su}	f_{su}, MPa	f_y, MPa	ε_{sh}	ε_{su}	f_{su}, MPa
C100B60N15	391	0.00773	0.127	637	494	0.01265	0.132	729	451	0.0065	0.109	716
C100B60N25	391	0.00773	0.127	637	494	0.01265	0.132	729	430	0.0106	0.142	661
C100B60N40	418	0.01273	0.138	675	467	0.01090	0.100	722	451	0.0065	0.109	716
C100B130N15	391	0.00773	0.127	637	494	0.01265	0.132	729	451	0.0065	0.109	716
C100B130N25	391	0.00773	0.127	637	494	0.01265	0.132	729	430	0.0106	0.142	661
C100B130N40	418	0.01273	0.138	675	467	0.01090	0.100	722	451	0.0065	0.109	716

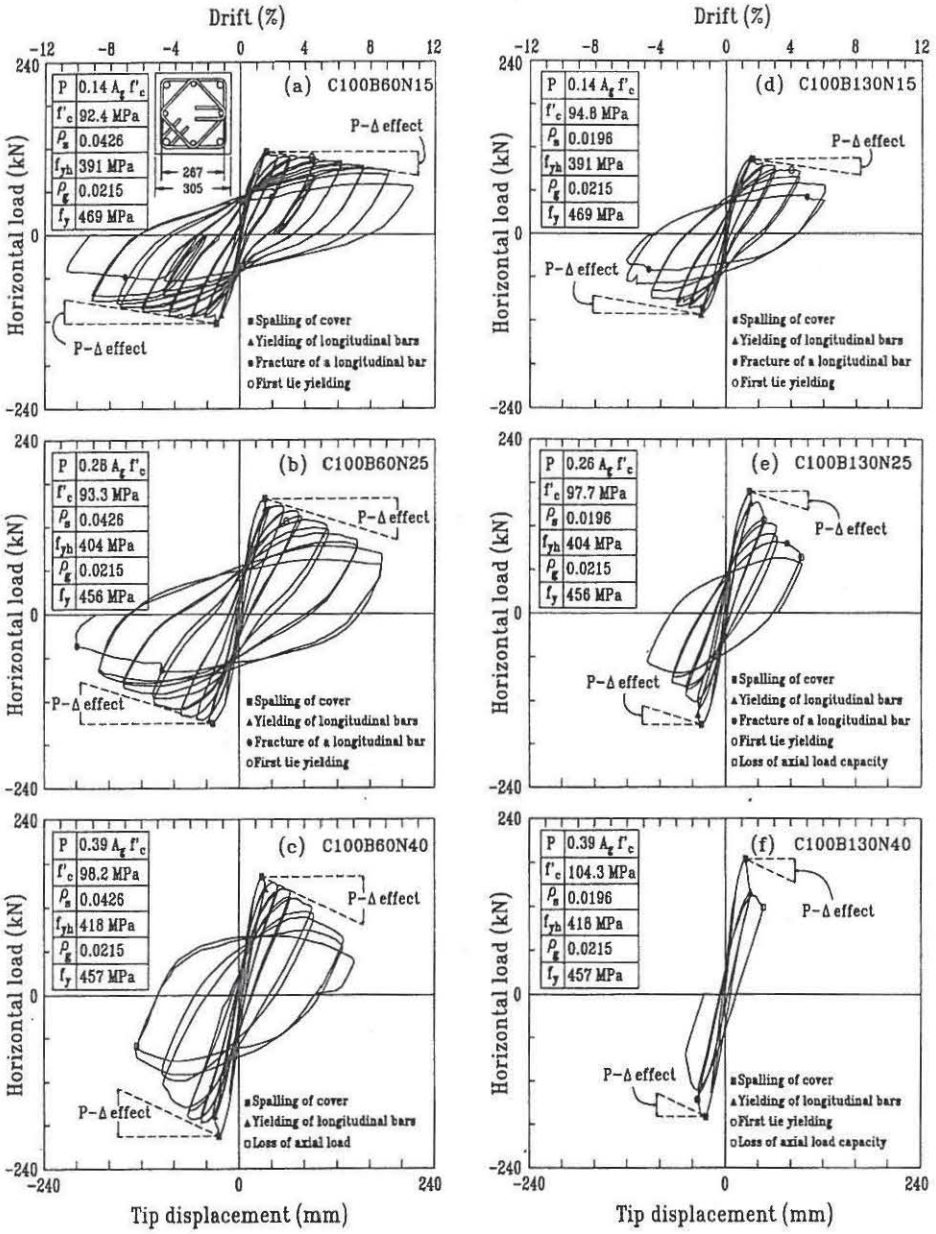

Fig. 5—Uncorrected lateral load versus tip displacement.

ported by four braced steel columns. The applied horizontal force was measured by the actuator load cell. The horizontal tip displacement was measured by an LVDT with a range of 300 mm. This LVDT was fixed to the laboratory strong-floor to eliminate the frame displacements from the measured column tip displacements. Displacement measurements were also taken from the actuator LVDT for test control while in displacement control mode. Due to the high frame stiffness, the difference between the actuator's LVDT and the independent LVDT was negligible.

The test began with the application of the axial load at the targeted value. For the first cycle of loading, the horizontal force reached 75% of the expected yield load. The second cycle reached the yield load and the yield displacement, defined as the point at which longitudinal bars first yield. Thereafter, each cycle was under displacement control with a maximum displacement equal to 1.5, 2, 3, ..., times the measured yield displacement up to failure (Fig. 4). Except for the first cycle, whose sole purpose was to crack the member to simulate real conditions and obtain elastic characteristics, all subsequent cycles were repeated twice. During the test, the axial load was maintained constant by re-adjusting the tension in the bars after each half cycle. All the experimental data were stored at predetermined steps and recorded at special occurrences such as cracking, yielding, and zero crossing. Acquisition was performed by increments of force and displacement triggers. The test ended when at least one of the three following events occurred:

1. The column was not able to sustain axial load, characterized by a 10% loss of axial load during a quarter of a cycle;
2. Flexural resistance dropped more than 50% of the maximum experienced capacity; and
3. A longitudinal bar ruptured, inducing a large drop of flexural capacity.

The end of the test did not correspond to conventional failure, which will be defined in following paragraphs, but rather to a point at which this conventional failure was certainly exceeded.

TEST RESULTS

General behavior

Figure 5 shows the applied lateral load versus tip displacement. The lateral load is reported as measured, and is not cor-

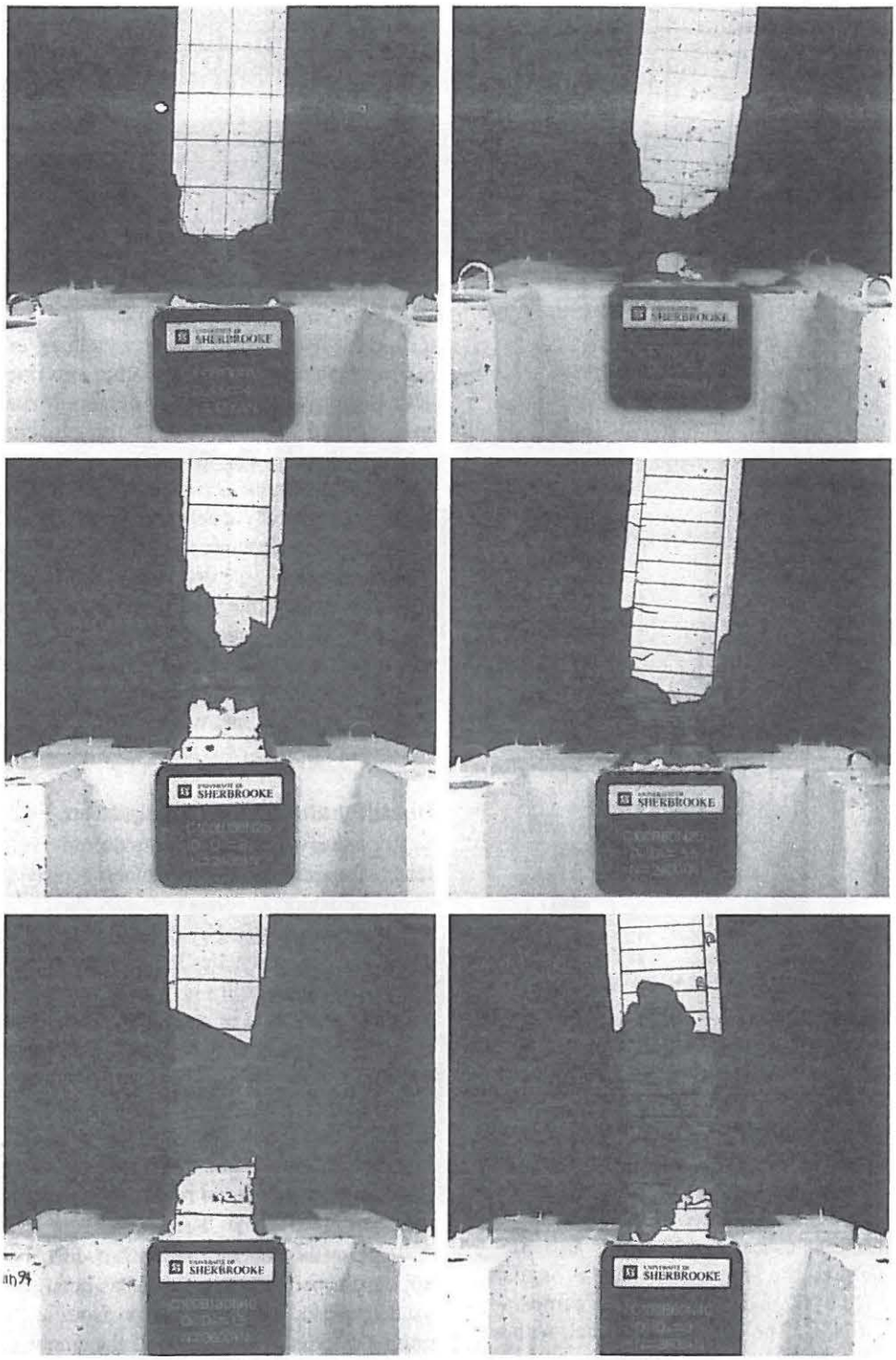

Fig. 6—Photographs of damaged regions and plastic hinge zones for all specimens.

rected for the P-Δ effect that is indicated by the dotted line. A strength gain occurs when the response curve, in absolute terms, lies above the oblique P-Δ dotted line. A strength loss is obtained when the response curve is under the P - Δ line. Occurrence of special events such as spalling of cover concrete, yielding of ties, yielding, and buckling of longitudinal bars is indicated in Fig. 5.

Table 3 summarizes the main variables for each specimen. In this table, f_c' is the measured concrete compressive strength determined on 150 x 300 mm cylinders; s is the spacing between transverse ties; ρ_s is the volumetric ratio of confinement steel to concrete core, measured center-to-center of perimeter tie; f_{yh} is the average yield strength of ties; $P/A_g f_c'$ is the ratio of applied constant axial load P and the concrete gross section capacity $A_g f_c'$; and P/P_0 is the ratio of applied load and the nominal concrete capacity $P_0 = 0.85 f_c'(A_g - A_{st}) + A_{st} f_y$. Table 3 summarizes the main indexes quantifying the specimen hysteretic behavior for each column. The meaning of each index will be discussed in the following paragraphs.

Following significant buckling of the longitudinal bars, Specimens C100B60N15, C100B130N15, C100B60N25, and C100B60N40 failed after rupture of the longitudinal bars under tension. The longitudinal bars in C100B60N40 and C100B130N40 buckled slightly as the concrete was crushed. C100B130N40 had two large diagonal cracks in the damaged zone and exhibited very brittle behavior. Figure 6 shows the

Table 3—Summary of test results

Specimen	f_c', MPa	s, mm	ρ_s, %	f_{yh}, MPa	$P/A_g f_c'$	P/P_0	M_{max}, kNm	$\mu_{\Delta u}$	$\mu_{\phi u}$	E_N	I_W	D_{EW}
C100B60N15	92.4	60	4.26	391	0.14	0.15	245.8	8.8	—	97.8	49.2	567.4
C100B60N25	93.3	60	4.26	404	0.28	0.30	326.3	8.2	26.9	75.8	39.0	379.6
C100B60N40	98.2	60	4.26	418	0.39	0.42	377.4	5.2	7.6	33.8	22.5	114.2
C100B130N15	94.8	130	1.96	391	0.14	0.15	225.0	4.4	—	16.3	13.5	39.7
C100B130N25	97.7	130	1.96	404	0.26	0.28	335.0	2.3	3.3	3.1	3.4	4.2
C100B130N40	104.3	130	1.96	418	0.37	0.40	372.6	1.6	2.9	4.2	3.3	5.6

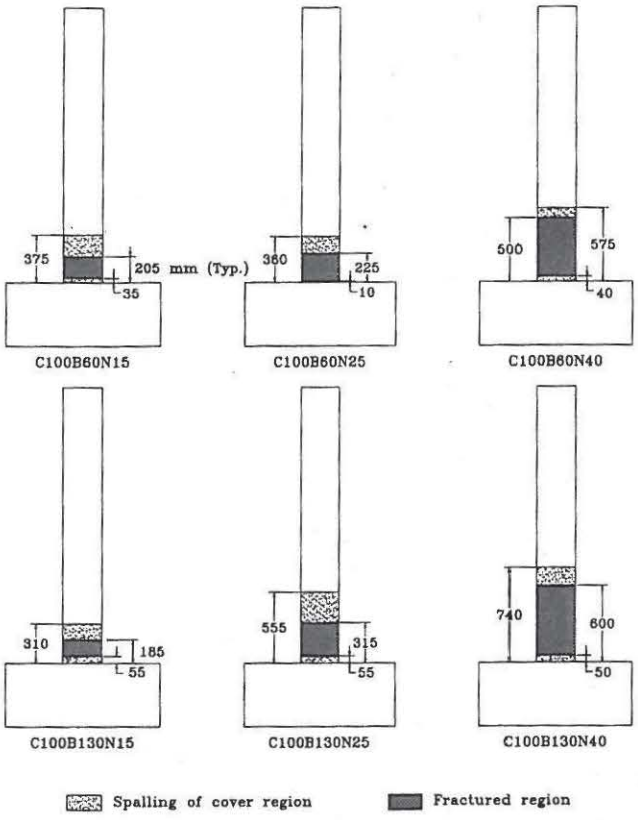

Fig. 7—Sketches of most damaged regions of specimens.

final appearance of the plastic hinge zone for all specimens at the end of the test. Figure 7 shows sketches of the most damaged regions for all specimens. All the columns were heavily damaged just above the base stub. The length of the damaged region increased with the axial-load level. This is also confirmed by strain readings on the longitudinal bars. A similar observation was reported by Watson and Park[10] on comparable specimens made of NSC. The authors noted that, with a 70% axial-load level, the damaged zone extended over three column depths and, for a 10% axial-load level, the damaged zone was approximately one column depth long. In all the specimens, however, regions just above the stub were not damaged, although they were subjected to the maximum moment (Fig. 7). The same phenomena were observed in similar specimens by other researchers.[4,5,11] Sheikh and Khoury[11] attributed such behavior primarily to confinement to the sections provided by the base stub in its immediate vicinity. Such confinement increases actual moment capacity of the sections just above the stub. This length of undamaged concrete corresponds to the spacing between the column-stub interface with the first hoop showing an average value of approximately 40 mm for all six specimens. Therefore, the resisting moment M'_{max} is calculated at 40 mm above the column-stub interface. For each column, M'_{max} is reported in Table 3.

The cover concrete of specimens C100B60N15 and C100B130N15 spalled off after yielding of the longitudinal reinforcement, while, for the other specimens, it spalled off before yielding. A loud noise occurred when the cover concrete spalled off suddenly, as the capacity of the column dropped sharply. This loss of capacity increased with axial load. In the case of C100B130N40, with a 37% axial-load level, the flexural capacity dropped almost 20%, while, for the companion Specimen C100B130N15, with an axial-load level of only 14%, the drop was about 5%. The specimens did not exhibit any warning signs, such as vertical cracking, prior to spalling. The splitting plane between cover and core concrete was found to be quite smooth due to cracks passing through the aggregate. No tie failed during the test. Though the maximum strain measured in ties was 0.011 m/m, average strains measured over all specimens ranged from 0.001 to 0.006 m/m.

Ductility and energy dissipation

To quantify the response of columns, it is desirable to define response indexes that quantitatively describe the columns' behavior. In seismic design, the inelastic deformation is generally quantified by ductility parameters and by energy dissipation capacity. For long-period structures, it has been stated that the ductility is directly related to the strength reduction factor used in most codes[12] to calculate the seismic base shear. The energy dissipation capacity is an important parameter in the design of short-period structures and structures subjected to a long-duration earthquake. The energy dissipation capacity also accounts for the history of loadings in addition to maximum displacement attained. Both types of indicators are computed in this paper to compare the column behavior on a rational basis.

Because the behavior of reinforced concrete structures is not elastic-perfectly plastic, it has been the general practice to define ductility parameters from a conventional diagram.[11,13] Hence, the load-displacement behavior is idealized as a bilinear diagram, constituted of an elastic branch and a inclined postelastic branch (Fig. 8(a)). The elastic branch is secant to the real curve at 75% of maximum horizontal load, and reaches the maximum horizontal load to define the yield displacement for Δ_{yI}. The failure of the column is conventionally defined at the postpeak displacement Δ_2, where the remaining capacity of the column has dropped to 80% of the peak load. The idealized postelastic branch starts at point (Δ_{yI}, H_{max}) and goes to (Δ_2, H_2). H_2 is defined such that the idealized diagram and the real envelope curve have the same area under the curve, ensuring equal energy criteria. The sectional behavior in terms of moment-curvature diagrams is idealized with the same procedure (Fig. 8(b)). The ductility parameters are defined from the idealized diagrams. The ultimate displacement ductility is defined as

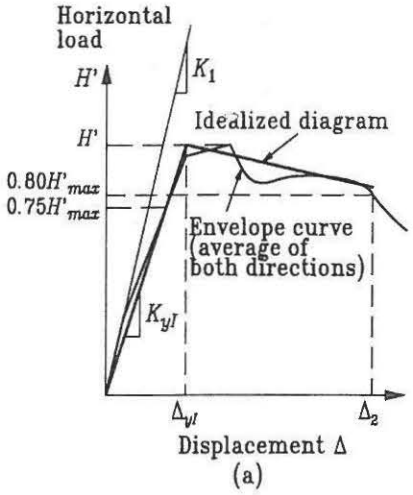

Fig. 8—Ideal curve definitions.

$$\mu_{\Delta u} = \frac{\Delta_2}{\Delta_{yI}} \tag{1}$$

and the ultimate curvature ductility

$$\mu_{\phi u} = \frac{\phi_2}{\phi_{yI}} \tag{2}$$

A column is generally considered ductile if displacement ductility ranges from 4 to 6. Table 3 provides the values of $\mu_{\Delta u}$ and $\mu_{\phi u}$ for each column. The main drawback in using the ductility parameters is a lack of general acceptance of a common definition in the research community for the yielding of a reinforced concrete member. The maximum interstory drift ratio δ_u is a simpler parameter to use and is based on the measured displacement at failure

$$\delta_u = \frac{\Delta_2}{z} \tag{3}$$

where z = 2000 mm is the column height. This parameter takes into account both inelastic and elastic behavior. It is generally assumed that a drift ratio of about 4% represents a very good level of ductility.[6]

The energy dissipation is defined for a cycle i by the hatched area in Fig. 9, or mathematically by

$$E_i = \oint_A^B F du \tag{4}$$

The total energy dissipated during the test until 80% conventional failure is

$$E_{hyst} = \sum_{i=1}^{n} E_i \tag{5}$$

where n is the number of cycles to failure. For comparison purposes, it is convenient to normalize the dissipated energy

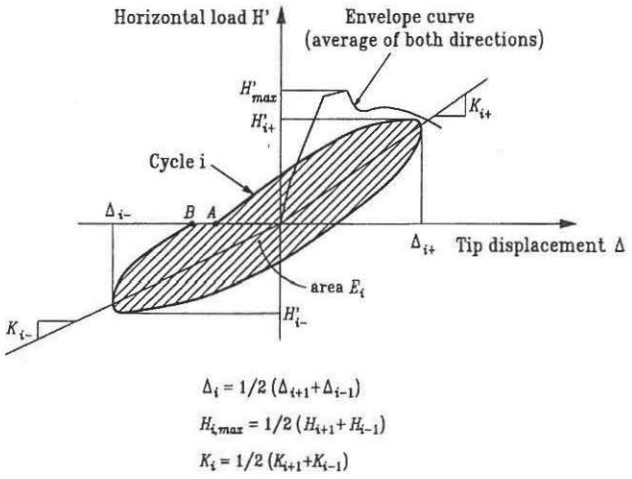

Fig. 9—Energy dissipation.

$$E_N = \frac{1}{H'_{max}\,\Delta_{yI}} \sum_{i=1}^{n} E_i \tag{6}$$

where E_N is the normalized dissipated energy. To determine E_N, only cycles occurring before conventional failure are taken into account. This data is provided for each specimen in Table 3.

Energy dissipation and inelastic deformation capabilities may also be assessed by the work and damage indexes. Gosain et al.[14] proposed the following work index

$$I_W = \sum_{i=1}^{n} \frac{H_i \Delta_i}{H'_{max}\,\Delta_{yI}} \tag{7}$$

This index has the great advantage of being easy to compute. Ehsani and Wright[15] introduced a damage index combining the cyclic dissipated energy and the elastic energy

$$D_{EW} = \frac{1}{H'_{max}\,\Delta_{yI}} \sum_{i=1}^{n} E_i \left(\frac{K_i}{K_{yI}}\right)\left(\frac{\Delta_i}{\Delta_{yI}}\right)^2 \tag{8}$$

where K_i and Δ_i are defined in Fig. 9. I_W and D_{EW} are computed for all the columns and reported in Table 3.

Table 4—Influence of level of axial load on main response indexes

Specimen	$P/A_g f_c'$	f_c', MPa	ρ_s, %	$\mu_{\phi u}$	$\mu_{\Delta u}$	$\delta_{\theta u}$	E_N	D_{EW}	I_W
Set no. 1									
C100B60N15	0.14	92.4	4.26	—	8.8	9.1	97.8	49.2	567.4
C100B60N25	0.28	93.3	4.26	26.9	8.2	8.7	75.8	39.0	379.6
C100B60N40	0.39	98.2	4.26	7.6	5.2	5.1	33.8	22.5	114.2
Set no. 2									
C100B130N15	0.14	94.8	1.96	—	4.4	4.6	16.3	13.5	39.7
C100B130N25	0.26	97.7	1.96	3.3	2.3	2.4	3.1	3.4	4.2
C100B130N40	0.37	104.3	1.96	2.9	1.6	1.5	4.2	3.3	5.6

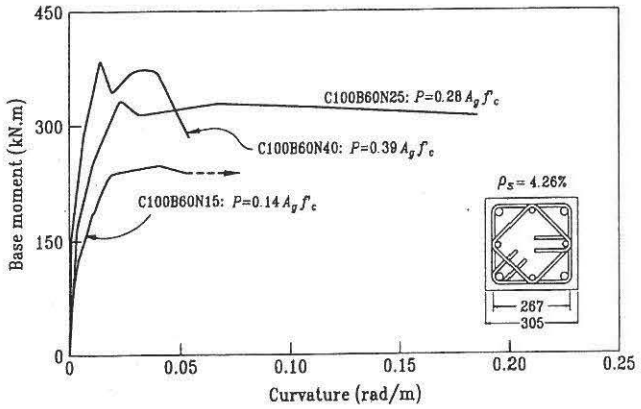

Fig. 10—Influence of axial-load level for columns with volumetric ratio of transverse steel of 4.26%.

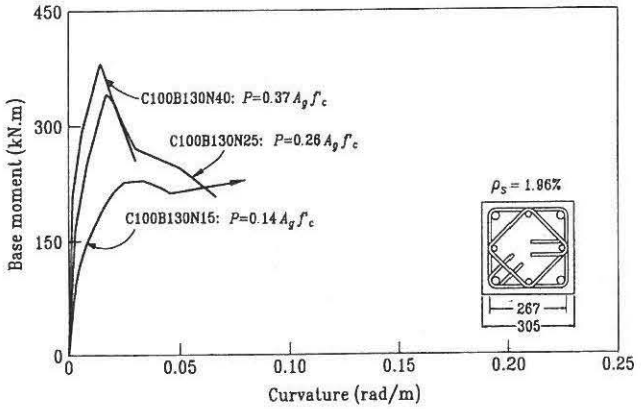

Fig. 11—Influence of axial-load level for columns with volumetric ratio of transverse steel of 1.96%.

ANALYSIS OF RESULTS

As mentioned previously, the effects of two variables are investigated in the present experimental program: 1) the effect of axial-load level; and 2) the volumetric ratio of transverse steel. It is possible to assess the effect of each variable graphically from Fig. 5. In this figure, the responses of the specimens are arranged in three rows and two columns. Specimens tested with the same target axial load are placed on the same row. Specimens with the same volumetric ratio and spacing of transverse reinforcement are placed in columns. The effect of axial-load level can be assessed by comparing diagrams in the same column; the influence of volumetric ratio of transverse steel can be assessed by comparing in the same row.

Effect of axial-load level

The influence of the axial-load level is assessed with two sets of three columns with the same volumetric ratio of confinement steel. The first set of columns consists of specimens C100B60N15, C100B60N25, and C100B60N40. The three specimens had the same 4.26% volumetric ratio of transverse steel, and were made with concrete of comparable strength. They were subjected to axial-load levels of 14, 28, and 39%, respectively. In Fig. 5, all three specimens' responses have been placed on the left column. The axial-load level increases from the top of the figure to the bottom. The specimens with the lowest axial-load level, C100B60N15, exhibited a very ductile behavior, as well as an excellent capacity to sustain large inelastic cyclic displacement. The ductility parameters and energy dissipation capacity for the three specimens are reported in Table 4. The displacement ductility drops from 8.8 to 8.2 to 4.7 when the axial-load levels increase from 14 to 28 to 39%, respectively. The same influence is observed on the other indicators: that is, the curvature ductility, the normalized dissipated energy E_N, the work index I_W, and the damage index D_{EW}. Figure 10 shows the influence of the axial-load level on the moment curvature envelope curves for the three columns. The arrow at the end of the response curve for Specimen C100B60N15 in this figure indicates that the curvature measurement stopped long before the end of the test, as stated previously. This figure indicates that, if the axial-load level has a beneficial influence on the moment resisting capacity, it has a negative effect on the inelastic cyclic behavior of the column.

The second set is composed of Specimens C100B130N15, C100B130N25, and C100B130N40. The three specimens have the same 1.96% volumetric ratio of transverse steel, and were made with concrete of comparable strength. They have been subjected to axial-load levels of 14, 26, and 37%, respectively. The transverse ties were spaced at 130 mm. In Fig. 5, the responses of the three specimens are all placed on the right column. The axial-load level increases from the top of the figure to the bottom. The column subjected to the lower level of axial load was able to sustain reasonable inelastic cyclic displacement. As the axial load increases, however, the behavior shows an insufficient level of ductility and energy dissipation capacity for seismic applications. The response indexes are reported in Table 4. The indexes show the same tendency to decrease as the level of axial load increases. Figure 11 reflects the influence of the axial-load level on the moment curvature envelope curves for the three columns. The arrow at the end of the response curve for Specimen C100B130N15 indicates that the curvature measurement stopped long before the end of the test, as stated previously. As for the previous three columns, this figure shows that the axial-load level has a beneficial effect on moment resisting capacity, but it has a negative influence on the inelastic behavior of the column.

Analysis of the results of this experimental program allow the authors to conclude that the level of axial load significantly affects column behavior. This has already been stated in the literature for NSC[2,10] and HSC.[3-5] The ACI Code for

Table 5—Influence of volumetric ratio of confinement steel on main response indexes

Specimen	ρ_s, %	f_c', MPa	$P/A_g f_c'$	$\mu_{\phi u}$	$\mu_{\Delta u}$	$\delta_{\theta u}$	E_N	D_{EW}	I_W
Set no. 1									
C100B130N15	1.96	94.8	0.14	—	4.4	4.6	16.3	13.5	39.7
C100B60N15	4.26	92.4	0.14	—	8.8	9.1	97.8	49.2	567.4
Set no. 2									
C100B130N25	1.96	97.7	0.26	3.3	2.3	2.4	3.1	3.4	4.2
C100B60N25	4.26	93.3	0.28	26.9	8.2	8.7	75.8	39.0	379.6
Set no. 3									
C100B130N40	1.96	104.3	0.37	2.9	1.6	1.5	4.2	3.3	5.6
C100B60N40	4.26	98.2	0.39	7.6	5.2	5.1	33.8	22.5	114.2

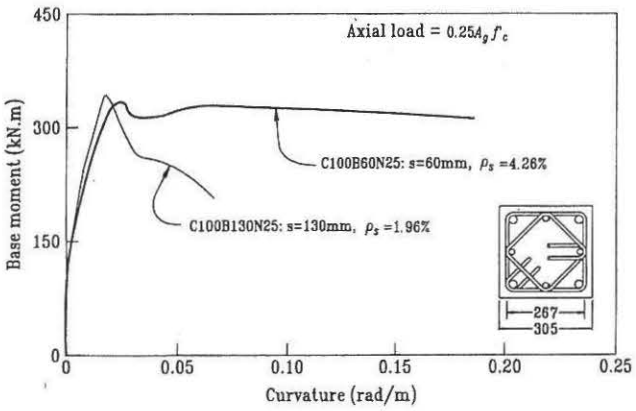

Fig. 12—Influence of volumetric ratio of transverse steel for columns subjected to axial-load level of 25%.

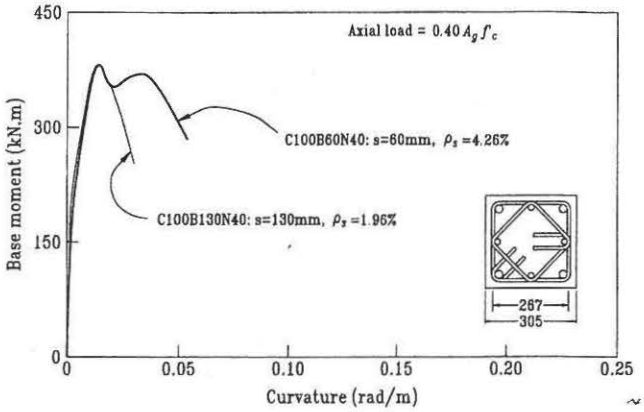

Fig. 13—Influence of volumetric ratio of transverse steel for columns subjected to axial-load level of 40%.

calculating confinement reinforcement still doesn't take this into account. Sheikh, Shah, and Khoury[2] state that the ACI confinement reinforcement requirements are not conservative in cases of highly axially loaded columns, and rather conservative and uneconomical in a great number of situations of practical interest in which columns support small axial compression. This is clearly illustrated through the experimental results presented in this paper. Indeed, Specimen C100B130N15 exhibits acceptable ductile behavior, even though it is made with HSC confined with less than 45% of the transverse reinforcement required by the ACI Code. On the other hand, Specimen C100B60N40, which complied with the ACI transverse reinforcement requirement, experienced similar behavior. For HSC to be used economically, the confinement reinforcement must be related to the level of axial load.

Effect of transverse reinforcement

The influence of the volumetric ratio of confinement steel is assessed on three sets of columns. The first set comprises C100B60N15 and C100B130N15. While both specimens are subjected to the same level of axial load, the volumetric ratio of confinement steel is 1.96% for C100B130N15, and 4.26% for C100B60N15. Figure 5 illustrates that Specimen C100B60N15 can sustain larger inelastic cyclic displacement than Specimen C100B130N15. The results presented in Table 5 indicate that Specimen C100B60N15 had a displacement ductility and ultimate drift ratio about twice that of Specimen C100B130N15. The dissipated energy and the damage index of Specimen C100B60N15 are approximately four times higher than for specimen C100B130N15; the work index is about 14 times higher. The second set comprises C100B60N25 and C100B130N25. Both specimens have the same transverse reinforcement as C100B60N15 and C100B130N15, respectively. Specimens in the second set, however, were subjected to an axial-load level targeted at 25% of $A_g f_c'$. Figure 5 reveals that Specimen C100B60N25 sustains larger inelastic cyclic displacement than Specimen C100B130N25. The same observation arises from Fig. 12, showing an envelope moment curvature diagram. The displacement ductility and the ultimate drift ratio of Specimen C100B60N25 are about four times higher than with C100B130N25, and energy dissipation parameters of C100B60N25 are significantly higher than for C100B130N25. The same observations are drawn from the examination of the responses (Fig. 5 and 13) and the ductility parameters, as well as from the energy dissipation capacity from the third set (Specimens C100B60N40 and C100B130N40).

This experimental program points to the influence of the volumetric ratio of confinement steel as a main parameter in controlling column response. As was stated previously, however, the level of axial load is also very important. For practical applications, the requirement for volumetric ratio of transverse steel should be related to the axial-load level. For the geometry of the columns tested in this research program, a volumetric ratio of confinement steel of approximately 2% seems acceptable to reach ductile behavior under an axial load less than or equal to 15% of axial-load capacity. For an axial-load level of 40% of $A_g f_c'$, a volumetric ratio of confinement steel of approximately 4% seems adequate. The need for confinement will be detailed in the following section.

Requirements for ductility

In seismic zones, structural members designed to behave ductilely should be well confined. Confinement steel is recommended in codes of practice by design equations setting minimum amounts of transverse reinforcement to ensure a certain level of ductility. An ideal equation would provide the same level of ductility for all columns regardless of loading, concrete strength, or transverse steel yield strength. As

Table 6—Link between required reinforcement by Eq. (5) and member ductility

Specimen (1)	f_c', MPa (2)	s, mm (3)	f_{yh}, MPa (4)	A_{sh}, mm^2 (5)	$P/A_g f_c'$ (6)	P/P_0 (7)	ACI (8)	ACI, % (9)	NZS‖ (10)	NZS, % (11)	$\mu_{\Delta u}$ (12)
C100B130N40*	104.3	130	418	341	0.37	0.40	826	41.3	1488	22.9	1.6
C100B130N25*	97.7	130	404	341	0.26	0.28	800	42.7	952	35.9	2.3
U4†	93.0	45	453	386	0.60	0.62	440	87.7	854	45.2	2.3
AS-7HT‡	102.0	94	542	341	0.45	0.48	450	75.7	948	36.0	3.1
ES-8HT‡	102.2	70	463	400	0.47	0.50	400	100.0	873	45.8	3.6
AS-5HT‡	101.8	90	528	483	0.45	0.48	441	109.4	933	51.8	4.0
D60-15-4-25/8-0.2P§	100.8	67	454	253	0.19	0.20	450	56.3	286	88.5	4.0
C100B130N15*	94.8	130	391	341	0.14	0.15	802	42.6	384	89.0	4.4
ES-1HT‡	72.1	95	463	400	0.50	0.50	383	104.5	800	50.0	4.6
AS-3HT‡	71.8	90	542	341	0.50	0.50	304	112.4	637	53.5	5.0
D60-15-3C-15/8-0.3P§	103.8	41	495	214	0.28	0.30	326	65.6	294	72.8	5.0
C100B60N40*	98.2	60	418	341	0.39	0.42	359	95.2	682	50.0	5.2
U2†	98.0	64	453	386	0.30	0.31	660	58.5	592	65.3	5.2
D60-15-3C-15/8-0.2P§	100.3	41	495	214	0.19	0.20	315	67.9	166	128.9	6.0
AS-2HT‡	71.7	90	542	341	0.36	0.36	303	112.5	416	82.1	6.2
AS-6HT‡	101.9	76	463	683	0.46	0.49	433	157.7	921	74.1	6.3
AS-4HT‡	71.9	100	463	683	0.50	0.50	402	169.9	839	81.4	7.0
C100B60N25*	93.3	60	404	341	0.28	0.30	353	96.8	437	78.1	8.2
C100B60N15*	92.4	60	391	341	0.14	0.15	361	94.6	176	193.7	8.8

*Specimen from present research program.
†Specimen from Li et al.[4]
‡Specimen from Bayrak and Sheikh.[5]
§Specimen from Azizinamini et al.[3]
‖New Zealand standard.

stated previously, this is not reflected by the ACI Code because Specimen C100B60N40, which complies with ACI Code requirements, has about the same behavior as Specimen C100B130N15, confined with less than 45% of the confinement steel required by the code. As demonstrated in this research program, axial load and volumetric ratio of transverse steel significantly affect column behavior, and must be included in code requirements. Watson, Zahn, and Park[16] proposed an equation for calculating the transverse steel reinforcement that accounts for axial-load level. Li et al.[4] showed that this equation is applicable to HSC columns. It was adopted in the New Zealand Standard[17] with some modifications. Under the New Zealand Code, the minimum effective area of confinement steel in one direction, A_{sh}, to reach ductile behavior is obtained from

$$A_{sh} = \frac{\left(1.3 - \rho_g \frac{f_y}{0.85 f_c'}\right) sh''}{3.3} \frac{A_g}{A_c} \frac{f_c'}{f_{yh}} \frac{P}{\phi f_c' A_g} - 0.006 sh'' \quad (9)$$

where h'' is the dimension of the concrete core measured outside the peripheral hoop; ϕ is the strength reduction factor (taken as 0.85 in this study); f_{yh} is the confining steel yield strength (which shall not be taken larger than 800 MPa); and f_c' is the concrete strength (not to exceed 70 MPa for ductile elements and elements with limited ductility).

At this point, it is interesting to consider all the available data on full-scale HSC columns to assess the use of the ACI Code and the New Zealand Standard equations. Data from various authors[3-5] are summarized in Table 6, along with the results of this research. Only the HSC columns confined by transverse reinforcement with yield strengths less than 550 MPa are accounted for. The problem of high yield strength steel is beyond the scope of this article, and will be discussed in a forthcoming paper. In this table, Column 5 gives the provided effective area of confinement steel A_{sh}; Columns 8 and 10 show the minimum confinement steel required by the ACI Code and the New Zealand Standard, respectively; Columns 9 and 11 present the provided area of confinement steel for each specimen in percentage of those required by the ACI Code and the New Zealand Standard, respectively. As there is no real consensus about the level of ductility for seismic design, and no widely accepted definition of ductility, it was decided not to classify the columns as ductile or not ductile. They were, however, ranked in order of increasing ductility. As confinement requirements should be related to the available ductility, the ratio between provided and required confinement steel should be linked to column ductility. The data in this table show that the ACI Code requirements do not always translate into ductile behavior. Column ES-8HT, with 100% of the ACI Code requirement, does not exhibit a good level of ductility, whereas Columns U2 and D60-15-3C-15/8-0.2P, with 58% and 68% of required transverse reinforcement by the ACI Code, respectively, display more ductility. Column C100B130N15 behaves ductilely with only 43% of the ACI Code required transverse steel.

The New Zealand Code requirements seem more rational. Generally, the ratio between provided and required confinement steel relates fairly well to the available displacement ductility. Some specimens with less confinement steel than required, however, behaved ductilely. This is the case with Specimens ES-1HT, AS-3HT, D60-15-3C-15/8-0.3P, C100B60N40, and U2, which exhibited a good level of ductility while having between 50% and 73% of the lateral reinforcement required by the New Zealand Standard.

This comparison appears to indicate that none of the current codes adequately provide for confining steel requirements that ensure a good level of ductility. The ACI Code requirements are too conservative in the case of low axial-load level, but not enough so in the opposite case. The New Zealand Standard requirements seem to be more appropriate, but are still not adequate for all the specimens. Although the New Zealand Standard requirements warrant revision, they appear more appropriate than the ACI Code for the moment.

CONCLUSION

This study provides new data on the behavior of six HSC columns subjected to combined constant axial compressive load and reversed cyclic flexure. It is shown that HSC can behave ductilely if:

1. The columns are subjected to low axial compression, even when confined with less transverse reinforcement than required by the ACI Code. It has been shown that approximately 50% of the ACI Code required reinforcement is necessary for a column subjected to an axial-load level of less than or equal to 15% of the gross axial-load capacity; and

2. The columns are very well confined (more than that required by the ACI Code requirements) when subjected to an axial-load level greater than 40% of the gross axial-load capacity.

Hence, HSC can be used in seismic zones, provided that it is adequately confined. The New Zealand Standard requirements were tested on 19 columns by different researchers, including the six columns tested in this research program. Although its requirements for transverse reinforcement to achieve a ductile behavior didn't account for the behavior of all the columns tested, it constitutes a step forward compared with the ACI Code requirements as it considers the influence of the axial-load level in transverse steel requirements.

The safe, economical use of HSC in seismic zones still depends on relating the required ductility to the confinement detailing and amount of transverse reinforcement. When the columns are subjected to a high axial-load level, a significant amount of lateral steel is necessary. Ratios exceeding 4% will be difficult to use in practice. High-yield strength steel may be a solution to reduce the quantities required. New equations should be developed that take into account high-strength transverse steel and axial-load level. In addition, research is needed to investigate the influence of important parameters such as slenderness ratio, stirrups spacing, and size effect.

ACKNOWLEDGMENTS

The financial assistance provided by the Natural Sciences and Engineering Research Council of Canada (NSERC) and by the Fonds pour la Formation de Chercheurs et L'aide à la Recherche of the Government of Quebec (FCAR) is gratefully acknowledged.

CONVERSION FACTORS

1 MPa = 145 psi
1 mm = 0.394 in.
1 kN = 0.2248 kips
1 kN-m = 0.738 kips-ft

NOTATIONS

A_c = cross-sectional area of concrete core measured center-to-center of outer tie
A_g = gross section of concrete
A_{sh} = total cross-sectional area of transverse reinforcement
A_{st} = total cross-sectional area of longitudinal reinforcement
E_c = modulus of elasticity of plain concrete
f_c' = maximum compressive strength of concrete measured from 150 x 300 mm cylinders
f_r = modulus of rupture of concrete
f_y = yield strength of longitudinal reinforcement steel
f_{yh} = yield strength of transverse reinforcement steel
f_{su} = ultimate strength of reinforcement steel
h'' = depth of concrete core measured out-to-out of peripheral hoop
H = applied horizontal load
P = axial load carried by concrete
P_0 = nominal axial-load capacity of column: $P_0 = 0.85 (A_g - A_{st}) f_c' + A_s f_y$
s = center-to-center spacing between sets of ties
Δ = tip displacement of column
Δ_2 = maximum tip displacement of column
Δ_{fy} = ideal yield displacement of column
ε_c' = axial strain in plain concrete corresponding to f_c'
ε_{sh} = commencement of strain hardening in steel bars
ε_y = strain in reinforcement steel at yield strength
ε_{su} = ultimate strain of reinforcement steel
$\mu_{\Delta u}$ = ultimate displacement ductility
$\mu_{\phi u}$ = ultimate curvature ductility
ρ_g = volumetric ratio of longitudinal reinforcement in column cross section
ρ_s = volumetric ratio of transverse reinforcement in concrete core measured center-to-center of ties
ϕ = curvature
ϕ_2 = maximum curvature
ϕ_{fy} = ideal yield curvature

REFERENCES

1. ACI Committee 318, "Building Code Requirements for Structural Concrete (ACI 318-95) and Commentary (ACI 318R-95)," American Concrete Institute, Farmington Hills, Mich., 1995, 369 pp.

2. Sheikh, S. A.; Shah, D. V.; and Khoury, S. S., "Confinement of High-Strength Concrete Columns," ACI JOURNAL, *Proceedings* V. 91, No. 1, Jan.-Feb. 1994, pp. 100-111.

3. Azizinamini, A.; Baum Kuska, S. S.; Brungardt, P.; and Hatfield, E., "Seismic Behavior of Square High-Strength Concrete Columns," *ACI Structural Journal*, V. 91, No. 3, May-June 1994, pp. 336-345.

4. Li, B.; Park, R.; and Tanaka, H., "Strength and Ductility of Reinforced Concrete Members and Frames Constructed Using High-Strength Concrete," *Research Report* No. 94-5, Department of Civil Engineering, University of Canterbury, Christchurch, New Zealand, 1994, 373 pp.

5. Bayrak, O., and Sheikh, S. A., "High-Strength Concrete Columns under Simulated Earthquake Loading," *Journal of Structural Engineering*, ASCE, V.124, No. 9, 1998, pp. 999-1010.

6. ACI-ASCE Committee 441, "High-Strength Concrete Columns: State of the Art," *ACI Structural Journal*, V. 94, No. 3, May-June 1997, pp. 323-335.

7. Cusson, D., and Paultre, P., "High-Strength Concrete Columns Confined by Rectangular Ties," *Journal of Structural Engineering*, ASCE, V. 120, No. 3, 1994, pp. 783-804.

8. Cusson, D., and Paultre, P., "Stress-Strain Model for Confined High-Strength Concrete," *Journal of Structural Engineering*, ASCE, V. 121, No. 3, 1995, pp. 468-477.

9. Paultre, P., and Légeron, F., "Seismic Behavior of High-Strength Concrete Tied Columns," *High-Strength Concrete,* Proceedings of the First International Conference, A. Azizinamini, D. Darwin, and C. French, eds., ASCE, Reston, Va., 1999, pp. 159-172.

10. Watson, S., and Park, R., "Simulated Seismic Load Tests on Reinforced Concrete Columns," *Journal of the Structural Division*, ASCE, V. 120, No. 6, 1994, pp. 1825-1849.

11. Sheikh, S. A., and Khoury, S. S., "Confined Concrete Columns with Stubs," *ACI Structural Journal*, V. 90, No. 4, Sept.-Oct. 1993, pp. 414-431.

12. Newmark, N. M., and Hall W. J., *Earthquake Spectra and Design*, Earthquake Engineering Research Institute, Berkeley, Calif., 1980, 103 pp.

13. Park, R., "Evaluation of Ductility of Structures and Structural Assemblages from Laboratory Testing," *Bulletin of the New Zealand National Society for Earthquake Engineering*, V. 22, No. 3, 1989, pp. 155-166.

14. Gosain, K. N.; Brown, H. R.; and Jirsa J. O., "Shear Requirements for Load Reversals on RC Members," *Journal of the Structural Division*, ASCE, V. 103, No. 7, 1977, pp. 1461-1476.

15. Ehsani, M. R., and Wright J. K., "Confinement Steel Requirements for Connections in Ductile Frames," *Journal of the Structural Division*, ASCE, V. 116, No. 3, 1990, pp. 751-767.

16. Watson, S.; Zahn F. A.; and Park, R., "Confining Reinforcement for Concrete Columns," *Journal of the Structural Division*, ASCE, V. 120, No. 6, 1994, pp. 1798-1824.

17. NZS 3101: Part 1: 1995, "Code of Practice for the Design of Concrete Structures," Standards Association of New Zealand, Wellington, New Zealand, 1995.

18. CSA Technical Committee, "Design of Concrete Structures for Buildings," CAN3-A23.3-M94, Canadian Standards Association, Rexdale, Ontario, 1994, 199 pp.